



LAWRENCE
LIVERMORE
NATIONAL
LABORATORY

ALLOYING-DRIVEN PHASE STABILITY IN GROUP VB TRANSITION METALS UNDER COMPRESSION

A. Landa, P. Soderlind, O. I. Velikokhatnyi, I. I.
Naumov, A. V. Ruban, O. E. Peil, L. Vitos

July 13, 2010

Physical Review B

Disclaimer

This document was prepared as an account of work sponsored by an agency of the United States government. Neither the United States government nor Lawrence Livermore National Security, LLC, nor any of their employees makes any warranty, expressed or implied, or assumes any legal liability or responsibility for the accuracy, completeness, or usefulness of any information, apparatus, product, or process disclosed, or represents that its use would not infringe privately owned rights. Reference herein to any specific commercial product, process, or service by trade name, trademark, manufacturer, or otherwise does not necessarily constitute or imply its endorsement, recommendation, or favoring by the United States government or Lawrence Livermore National Security, LLC. The views and opinions of authors expressed herein do not necessarily state or reflect those of the United States government or Lawrence Livermore National Security, LLC, and shall not be used for advertising or product endorsement purposes.

Alloying-Driven Phase Stability in Group VB Transition Metals under Compression

A. Landa¹, P. Söderlind¹, O.I. Velikokhatnyi², I.I. Naumov³, A.V. Ruban⁴, O.E. Peil^{4,5},
and L. Vitos^{4,6}

¹Condensed Matter and Materials Division, Physical and Life Sciences Directorate,
Lawrence Livermore National Laboratory, Livermore, CA 94551, USA

²Department of Bioengineering, University of Pittsburgh, Pittsburgh, PA 15261, USA

³Information and Quantum Systems Laboratory, Hewlett-Packard, Palo Alto, CA 94304,
USA

⁴Department of Materials Science and Engineering, Applied Materials Physics, Royal
Institute of Technology, SE-100 44 Stockholm, Sweden

⁵Institute of Theoretical Physics, University of Hamburg, 20355 Hamburg, Germany

⁶Department of Physics and Materials Science, Division for Materials Theory, Uppsala
University, SE-75121 Uppsala, Sweden

The change in phase stability of Group VB (V, Nb, and Ta) transition metals due to pressure and alloying is explored by means of first-principles electronic-structure calculations. It is shown that under compression stabilization or destabilization of the ground-state body-centered cubic phase of the metal is mainly dictated by the band-structure energy that correlates well with the position of the Kohn anomaly in the transverse acoustic phonon mode. The predicted position of the Kohn anomaly in V, Nb, and Ta is found to be in a good agreement with data from the inelastic x-ray or neutron scattering measurements. In the case of alloying the change in phase stability is defined by the interplay between the band-structure and Madelung energies. Alloying with a

small amount of a neighboring metal can either stabilize or destabilize the body-centered cubic phase relative to a phase with lower symmetry. We show that band-structure effects determine phase stability when a particular Group VB metal is alloyed with its nearest neighbors within the same d -transition series. In this case, the neighbor with less (to the left) and more (to the right) d electrons, destabilize and stabilize the body-centered-cubic phase, respectively. When V is alloyed with neighbors of a higher ($4d$ - or $5d$ -) transition series, both electrostatic Madelung and band-structure energies stabilize the body-centered-cubic phase. The opposite (destabilization) happens when Nb or Ta is alloyed with neighbors of the $3d$ -transition series.

I. INTRODUCTION

Recently Bosak *et al.* [1], using inelastic x-ray scattering technique, reported several anomalies in the phonon dispersion curve for V along high-symmetry directions. Among these anomalies was an upward bending of the transverse acoustic (TA) mode along the Γ - H direction, $[\xi 00]$, around $\xi = 0.24$. This peculiarity was early predicted in several theoretical studies [2-4]. Vanadium metal has been the subject of numerous experimental and theoretical studies due to its high superconducting transition temperature. Ishizuka *et al.* [5] found that for V the superconducting transition temperature, $T_c = 5.3$ K, increases linearly with pressure reaching 17.2 K (the highest T_c among the elemental metals reported so far) at 1.2 Mbar. In addition, they also found a small step-like increase in T_c near 600 kbar. In order to explore the possibility of a structural phase transition, Suzuki and Otani [2] performed first-principles calculations of the lattice dynamics of V in the pressure range up to 1.5 Mbar. They found that the

frequencies of the TA mode $[\xi 00]$ soften around $\xi = 1/4$ with increasing pressure and become imaginary (unstable) at pressures higher than 1.3 Mbar, indicating a structural phase transition. The recent synchrotron x-ray diffraction measurements on V [6] reported a new rhombohedral (*rh*) phase around 630-690 kbar that is in the same pressure range where a small step-like increase in T_c was observed [5]. Later theoretical studies confirm this finding and also suggest vanadium to return to the body-centered-cubic (bcc) phase around 2.5 – 3.2 Mbar [3, 4, 7, 8].

In the long wave-length limit ($q \rightarrow 0$) the trigonal shear elastic constant (c_{44}) is related to the TA $[\xi 00]$ phonon frequency, $\omega(q)$, by a simple relation: $\rho\omega^2(q)/q^2 \rightarrow c_{44}$. Landa *et al.* [9] found that the pre-martensitic softening of the TA $[\xi 00]$ phonon mode of V, predicted in Ref. [2] and later experimentally confirmed in Ref. [1], is attributed to the existence of parallel pieces of the Fermi surface (FS) which causes a strong electronic response at the nesting wave-vector that translates these pieces one to the other. They [9] also found that the nesting vector q_n , spanning two flat pieces of the FS in the 3rd band, already exists at zero pressure and leads to the Kohn anomaly in the TA $[\xi 00]$ phonon mode for small $q_n \approx 0.24(2\pi/a)$, where a is the lattice constant. According to the above mentioned relation between the TA $[\xi 00]$ phonon frequency $\omega(q)$ and trigonal shear elastic constant c_{44} , the Kohn anomaly also softens this elastic constant making it negative in the pressure range 1.80-2.75 Mbar. The full potential linear muffin-tin orbitals [10] and projector augmented waves [11] calculations reveal the lower limit of this pressure interval as 1.2 and 0.8 Mbar, respectively. Verma and Modak [4] emphasized that the transition from the bcc to *rh* structure in V under compression could occur even before the trigonal shear elastic constant becomes negative. They noticed that

the atomic displacement pattern related to the TA mode corresponds to rhombohedral distortion of the cubic structure and a reduction of the frequencies of TA modes under compression. The latter implies that the rhombohedral distortion becomes favorable under pressure, which leads to the splitting of the t_{2g} electronic states and consequently a reduction of the total energy through the Jahn-Teller (J-T) mechanism. They also came to the conclusion that a strong coupling exists between the t_{2g} electrons and TA mode phonons that increases with pressure and leads to a structural phase transformation from the bcc to *rh* at about 0.6 Mbar through the band J-T effect. A similar conclusion was independently derived by W. Luo, *et al.* [3].

The remaining Group VB transition metals, Nb and Ta, also represent the so-called hard superconductors [12] whose superconducting properties highly depend on their physical and chemical state. Nb has the highest superconducting transition temperature, $T_c = 9.25$ K, among the elemental metals at ambient pressure [13]. According to Matthias *et al.* [14], Ta becomes a superconductor at $T_c \sim 3.39$ -4.48 K. By using inelastic neutron scattering, Nakagawa and Woods [15] found a decrease (below the elastic constant line) in TA $[\xi 00]$ phonon frequencies for Nb around $\xi = 0.20$ (compare with $\xi = 0.24$ for V). This behavior of Nb was later confirmed by Sharp [16]. Varma and Weber [17] pointed out the importance of understanding the coexistence of high- T_c and phonon anomalies. Using the nonorthogonal tight binding representation for the d -electron contribution to the dynamic matrix, they were able to reproduce the negative curvature in the TA $[\xi 00]$ phonon branch for Nb. Woods [18] performed the frequency-wave-vector dispersion relation measurements in Ta using the inelastic neutron scattering technique similar that was used in measurements for Nb [15]. His

results showed strong analogies with previously measured Nb [15], however, a drastic decrease below the elastic constant line for TA [$\xi 00$] phonon mode, observed for Nb, was not detected. This observation allowed him to conclude that the trigonal shear elastic constant for tantalum metal should be significantly higher than for niobium. Thirty years later, Sacchetti *et al.* [19] performed neutron scattering measurements of the TA [$\xi 00$] phonon mode in Ta at temperature below 4.2 K and got the dispersion curve that is very similar to the one measured by Woods [18] at room temperature.

The softening of the trigonal shear elastic constant of Nb under compression was previously reported [9-11]. In analogy with V, Landa *et al.* [9] connected this phenomenon in Nb to the intra-band nesting, spanning significantly smaller pressure range than in the case of V. However, due to the lack of reliable experimental data on the phonon dispersions in V at that time, they could not use the results of their electron susceptibility calculations to verify the existence of the anomaly in the TA [$\xi 00$] phonon branch previously predicted for V in Ref. [2]. Neither did they perform this analysis for Nb although the inelastic neutron scattering measurements of the phonon dispersions have been available [15] for a long time. Now, when the inelastic x-ray scattering measurements provide very accurate phonon dispersions for V [1], it is time to fill this gap and verify the existence of the Kohn anomaly on the TA [$\xi 00$] phonon branch of V, Nb, and Ta.

Another task of this paper is to expand the study recently performed by Landa *et al.* [20] on stability in bcc transition metals due to alloying. In that letter the phase stability of Group VB (V, Nb, and Ta) transition metals was explored by first-principles electronic-structure calculations. We found that alloying with a small amount of a

neighboring metal can either stabilize or destabilize the body-centered-cubic relative to a lower symmetry rhombohedral phase. It was shown that band-structure effects determine phase stability when a particular Group VB metal is alloyed with its nearest neighbor within the same d -transition series. In this case, the neighbor with less (to the left) and more (to the right) d electrons destabilize and stabilize bcc, respectively. It was also found that when $3d$ -V is alloyed with neighbors of higher d -transition series, the electrostatic Madelung energy dominates and stabilizes the bcc phase. In the present paper we study how the phase stability of $4d$ -Nb changes when it is alloyed with neighbors of lower $3d$ - (Ti, V, or Cr) or higher $5d$ - (Hf, Ta, or W) metals. We also study what happens if $5d$ -Ta is alloyed with neighbors of lower $3d$ - and $4d$ - transition metals.

Our paper is organized as follows. Pertinent detailed of computation methods are described in section 2 followed by results of the generalized susceptibility calculations for transition metals (V, Nb, and Ta) in Section 3. Stability of the bcc alloys based on the VB transition metals is discussed in Section 4. We present our general discussion and conclusions in Section 5.

II. THEORETICAL BACKGROUND

In analogy with our previous papers [9, 10, 20], we employ two complementary techniques, EMTO and FPLMTO (see below). The calculations that we have referred to as exact muffin-tin orbitals (EMTO) are performed using a scalar-relativistic Green function technique based on an improved screened Korringa-Kohn-Rostoker method [21]. For the exchange/correlation approximation, we use the generalized gradient approximation [22]. In order to treat compositional disorder the EMTO method is

combined with the coherent potential approximation [23]. The calculations are performed for a basis set including valence *spdf* orbitals, whereas the core states are recalculated at each iteration. Integration over the irreducible wedge of the Brillouin zone (IBZ) is performed using the special *k*-points method [24] with 819 *k*-points for the bcc lattice. The Green function has been calculated for 60-80 complex energy points distributed exponentially on a semicircle with 3.0-4.1 Ry diameter enclosing the occupied states. These calculations include the on site screened Coulomb potential and energy, which take care of the electrostatics in the single-site DFT approximation [25]. The corresponding screening constants have been obtained in the locally self-consistent Green function (LSGF) [26] calculations for a 1024 atoms supercell that models the random equiatomic alloys. The equilibrium density and EOS are obtained from a Murnaghan fit [27] to the total energy versus the lattice constant curve. For the determination of the trigonal shear elastic constant, c_{44} , we apply a volume-conserving monoclinic distortion [28] and calculate the internal energy response. This setup requires 17457 *k*-points to perform integration over IBZ. The ground state for the *rh* phase is obtained by applying a volume conserving rhombohedral distortion [7] with 12100 *k*-points to perform integration over IBZ.

The generalized susceptibility of non-interacting electrons ($\chi(q)$) is selected in order to detect the FS nesting. This function is calculated by using the highly precise analytic tetrahedron method [29]. In order to reach high precision in the $\chi(q)$ calculations, the IBZ lattice is divided into 16000 tetrahedra.

For comparison and analysis, we also perform full-potential linear muffin-tin orbital (FPLMTO) [30] calculations for the elements and for alloys within the virtual

crystal approximation (VCA). In VCA the alloy system is modeled by a fictitious metal with atomic charge and valence corresponding to the concentration average between two neighboring elements. In this approach the alloying is modeled by the change of the valence electron population and it thus mostly address the effects of changes in the band energy. As in the case of the EMTO method, GGA is applied for the electron exchange-correlation approximation. 150 and 1620 k-points are used to perform integration over IBZ in calculations for the bcc lattice and trigonal shear elastic constant.

III. GENERALIZED SUSCEPTIBILITY CALCULATION

Figure 1 shows the partial (due to the $3^{\text{rd}} \rightarrow 3^{\text{rd}}$ electron intra-band transition, see Ref. [9, 10] for details) contribution to the generalized susceptibility, $\chi(q)$, of V, Nb, and Ta calculated along Γ -H ($\xi 00$) direction at ambient pressure. As can be seen from this plot, the generalized susceptibility has a peak (due to the intra-band nesting [9, 10]) at $\xi \approx 0.24$, 0.16, and 0.28 for V, Nb, and Ta, respectively, indicating the position where the Kohn anomaly on the TA [$\xi 00$] phonon branch is likely to occur. One can also see that this peak is more pronounced for V and Nb than for Ta suggesting that the Kohn anomaly is weaker in Ta than in V and Nb. In order to verify these results, we plot in Figure 2 the experimental phonon dispersion TA curve in [$\xi 00$] direction using numerical data on the phonon frequencies from Refs. [18, 31, and 32] for Ta, V, and Nb, respectively. The location of the peak on the partial generalized susceptibility curve at ambient pressure, presented in Figure 1, is marked by an arrow in Figure 2. One can see that the position of the calculated peak in $\chi(q)$ is in fair accord with the point of the maximum deviation below the elastic constant line of the experimental TA [$\xi 00$] phonon branch (the so-called

phonon softening). In comparison with V, this deviation is observed to a larger and smaller extent for Nb and Ta, respectively.

Tracing the change of the position of the maximum on the generalized partial susceptibility curve presented in Figure 3, we can plot (Figure 4) the magnitude of the nesting vector, or the position of the Kohn anomaly, as a function of pressure. Our calculations show that the nesting vector decreases as pressure increases and the termination of a so-called ‘jungle-gym’ (J-G) hole-tube [9, 10] occurs at between 2.25-2.50, 0.60-0.75, and 2.50-2.75 Mbar for V, Nb, and Ta respectively that is in a good agreement with results of Koči, *et al.* [11] for V and Nb, although their calculations reveal a lower termination pressure for Ta (~ 2.25 Mbar). However, one should remember that if in Ref. [11] the magnitude of the nesting vector was defined by measurements of the distance (a common normal) between the parallel sheets of the FS, our study defined this value numerically through the generalized susceptibility calculations. As was pointed in Ref. [9, 10], as soon as the nesting vector turns to zero, the electronic topological transition (ETT), when the neck between two electronic sheets of the FS appears (the J-G hole tube terminates at the [100] direction), takes place. Qualitatively, it is analogous to the event when the FS touches the BZ boundary and is always accompanied by a minimum or inflection in the shear elastic constants [33].

The softening of the trigonal shear elastic constant of V and Nb up to the ETT pressure was confirmed in Ref. [9-10]. According to Söderlind and Moriarty [34] (Figure 6), Cohen and Gülseren [35], Gülseren and Cohen [36] (Figure 1), and Koči, *et al.* [11] (Figure 1) ETT should take place for Ta at approximately 1.5-2 Mbar. Present calculations give a higher value (~ 2.5 Mbar).

IV. STABILITY OF THE BCC ALLOYS BASED ON THE V, Nb, AND Ta

Figure 5 shows calculated (FPLMTO) pressure dependence of the trigonal shear elastic constant, c_{44} , in V, Nb, and Ta [20]. For vanadium, c_{44} initially increases with pressure as to be expected for a stable phase, but close to 0.2 Mbar it drastically decreases. We predict the phase transition to the rh phase at 0.6 Mbar, close to the observed 0.6-0.7 Mbar [6]. For Nb a similar behavior is observed with the shear constant reaching a low minimum close to 0.5 Mbar before rising again. In Ta the softening is less severe but apparent between 0.5-0.8 Mbar.

For V our calculations predict a phase transition to the rh phase at 0.6 Mbar that abruptly changes its rhombohedral angle close to 1.1 Mbar before returning to bcc at 3.1 Mbar [20]. In Figure 6 we display the EMTO-CPA total energy as a function of rhombohedral distortion for V and its alloys with 5 at. % of Ti, Cr, and Nb [20]. Here the atomic volume is kept at $\Omega = 8.056 \text{ \AA}^3$ corresponding to a pressure of ~ 2.4 Mbar. Notice that pure V is unstable with respect to the distortion and alloying with a small amount of its left neighbor Ti increases the instability. Adding a small fraction of Cr or Nb, however, promotes the bcc phase which becomes stable for ~ 5 at. % Nb and ~ 11 at. % Cr (not shown). Our calculations also predict that Zr (~ 3 at.%), Mo (~ 5 at.%), Hf (~ 5 at.%), Ta (~ 5 at.%), and W (~ 4 at.%) stabilize the bcc phase of V at all pressures [20]. Thus all the metals in Group IVB, VB, and VIB prevent the rhombohedral phase in V, except Ti, which in contrast favors the distorted phase. Both EMTO-CPA and FPLMTO-VCA calculations [20] confirm that the band-filling argument (the number of valence electrons) is responsible, exclusively, for stabilization or destabilization of the bcc phase

when V is alloyed with its nearest neighbors within the same $3d$ -transition series, Cr or Ti, respectively. Stabilization of the bcc phase of V by alloying with neighbors of higher d -transition series was explained in Ref. [20] due to the dominance of the electrostatic Madelung energy contribution to the total energy, although only results for Nb as the dopant were presented. Below we consider 5 remaining dopants from the $4d$ - and $5d$ -transition series: Zr, Mo, Hf, Ta, and W.

Within the EMTO formalism, the total energy, E_{tot} , can be expressed as the sum of two contributions: $E_{tot} = E_I + E_M$, where E_I consists of all “local” (band-structure) contributions, $E_I = E_s + E_{intra} + E_{xc}$, such as the kinetic energy of non-interacting electron gas, E_s , the intra-cell electrostatic energy, E_{intra} , which is due to the electron-electron and electron-ion Coulomb interactions and also includes the screened Coulomb interactions in the case of the DFT-CPA calculations, and the exchange and correlation energy, E_{xc} . The remaining contribution, E_M , is the inter-cell Madelung energy.

Table 1 lists the total-energy response ΔE_{tot} and its contributions, ΔE_I and ΔE_M to a 1 % monoclinic deformation, used for the trigonal shear elastic constant c_{44} calculations [28], calculated for V and the $V_{95}Ti_{05}$, $V_{95}Cr_{05}$, $V_{95}Zr_{05}$, $V_{95}Nb_{05}$, $V_{95}Mo_{05}$, $V_{95}Hf_{05}$, $V_{95}Ta_{05}$, and $V_{95}W_{05}$ alloys at the same atomic volume $\Omega = 8.056 \text{ \AA}^3$. Negative values of the total-energy changes indicate mechanical instability of the bcc phase. Adding Ti to V slightly decreases ΔE_{tot} signaling further bcc destabilization and the change in E_I plays the dominant role. For the $V_{95}Cr_{05}$ alloy, again E_I is dominant, now having the opposite effect while the Madelung part remains nearly the same. Consequently, ΔE_{tot} increases and approaches zero with a near stabilization of the bcc phase. Adding of an additional 6 at. % of Cr in fact dictates the bcc phase for all pressures in V.

Adding 4*d*-transition metals (Zr, Nb, or Mo) to V significantly increases ΔE_{tot} thus implying stabilization of the bcc structure in the $V_{95}Zr_{05}$, $V_{95}Nb_{05}$, or $V_{95}Mo_{05}$ alloys. Notice that the increase in ΔE_I for the $V_{95}Nb_{05}$ alloy in comparison with pure V, which is mostly due to band-structure effects, is rather insignificant (+0.0059 mRy) and the main reason for stabilization of the bcc structure in this alloy is instead the increase in the electrostatic Madelung energy, ΔE_M , (+0.0282 mRy). However, for the $V_{95}Zr_{05}$ and $V_{95}Mo_{05}$ alloys the increase in ΔE_I is +0.0146 mRy and +0.0155 mRy, respectively, that, on average, is 2.55 times larger than that for the $V_{95}Nb_{05}$ alloy. Although the increase in ΔE_M , which is proportional to the magnitude of the charge transfer on the vanadium atoms (see Table 2), is significant: +0.0119 mRy, +0.0282 mRy, and +0.0301 mRy for the $V_{95}Mo_{05}$, $V_{95}Nb_{05}$, or $V_{95}Zr_{05}$ alloys, respectively, the increase in ΔE_I for the $V_{95}Mo_{05}$ alloy (+0.0155 mRy) is even larger than the increase in ΔE_M (+0.0119 mRy). So we can no longer credit the electrostatic Madelung energy as the dominating factor in stabilization of the bcc structure in the V-4*d*-transition metal alloys as suggested in Ref. [20].

Adding 5*d*-transition metals (Hf, Ta, and W) also stabilizes the bcc structure in the $V_{95}Hf_{05}$, $V_{95}Ta_{05}$, or $V_{95}W_{05}$ alloys. Although the increase in ΔE_M (+0.0095 mRy, +0.0183 mRy, and +0.0224 mRy, for the $V_{95}W_{05}$, $V_{95}Ta_{05}$, or $V_{95}Hf_{05}$ alloys, respectively), which is proportional to the magnitude of the charge transfer on the vanadium atoms (see Table 2), plays an important role in stabilization of the alloys, a significant increase in ΔE_I (+0.0086 mRy, +0.0348 mRy, and +0.0079 mRy, for the $V_{95}W_{05}$, $V_{95}Ta_{05}$, or $V_{95}Hf_{05}$ alloys, respectively) takes place indicating that increase in ΔE_M and ΔE_I is compatible for the $V_{95}W_{05}$ alloy. However, for the $V_{95}Ta_{05}$ alloy the

increase in ΔE_I is almost twice as large as that in ΔE_M . It appears that for only one alloy that V forms with $5d$ -transition metals under consideration, $V_{95}Hf_{05}$, the electrostatic Madelung energy is the major factor in stabilization of the bcc structure.

As mentioned above, small amounts (~ 3 -5 at. %) of $4d$ and $5d$ metals are enough to stabilize the bcc structure of V. For these alloys the Madelung energy plays an important role in the stabilization, as opposed to the V-Ti and V-Cr alloys where it is negligible. This contrasting behavior is due to the inherent difference between $4d$ and $5d$ states compared to the $3d$ states. The former are more extended in space as are their corresponding charge distribution. Consequently, there is a larger charge transfer when V is alloyed with a $4d$ or $5d$ metal than with its neighbors Ti and Cr. As can be seen from Table 2, the large and positive charge transfers means that more charge is supplied into the interstitial region thereby increasing the Madelung energy of the crystal that favors higher symmetry structures. Let us note that an addition of $4d$ - or $5d$ -metal dopants also affects the band-structure energy, due to the fact that they provide stronger hybridization but, as one can see from Table I for the case of V alloyed by Zr, Nb, and Hf, this effect is not as important as the change in the Madelung energy, but becomes compatible with the latter for the case of V alloyed with W and Mo, and even plays the dominant factor for the bcc structure stabilization in the V-Ta alloys.

The band-structure energy is also responsible for the pressure-induced shear softening in Nb at ~ 0.5 Mbar (Figure 5). Hence, there is an interest to explore the stability of bcc Nb with alloying. To this end we calculated the energy change in pure bcc Nb, and its alloys with $3d$ neighbors ($Nb_{95}Ti_{05}$, $Nb_{95}V_{05}$, and $Nb_{95}Cr_{05}$), $4d$ neighbors ($Nb_{95}Zr_{05}$, and $Nb_{95}Mo_{05}$), and $5d$ neighbors ($Nb_{95}Hf_{05}$, $Nb_{95}Ta_{05}$, and $Nb_{95}W_{05}$) caused

by 1 % of the monoclinic deformation. Calculations are performed at the same atomic volume $\Omega = 14.92 \text{ \AA}^3$ corresponding to a pressure of ~ 0.5 Mbar and the results are presented in Table 3. In Table 4 we summarize the calculated charge transfers for Nb alloyed with the members of Group IVB, VB, and VIB. As one can see from Table 4, there is a significant negative charge transfer on the Nb atoms when Nb is alloyed with 3d metals (Ti, V, and Cr). The large and negative charge transfers means that less charge is supplied into the interstitial region thereby decreasing the electrostatic Madelung energy contribution. The decrease in ΔE_M of pure Nb due to the alloying is proportional to the absolute value of the charge transfer and appears to be -0.0091 mRy, -0.0101 mRy, and -0.0144 mRy for the Nb₉₅Ti₀₅, Nb₉₅V₀₅, and Nb₉₅Cr₀₅ alloys, respectively. There is also a decrease in ΔE_I due to alloying: -0.0080 mRy, -0.0045 mRy, and -0.0036 mRy for the Nb₉₅Ti₀₅, Nb₉₅V₀₅, and Nb₉₅Cr₀₅ alloys, respectively, but in contrast to ΔE_M behavior, the drop in ΔE_I decreases as the absolute value of the charge transfer on the Nb atoms increases. Both the electrostatic Madelung and band-structure contributions determine the decrease in the total energy, ΔE_{tot} , of Nb when it is alloyed with 3d-transition metals, but only for the Nb₉₅Ti₀₅ alloy these contributions are comparable in magnitude and the ΔE_M contribution plays the decisive role in destabilization of the Nb₉₅V₀₅, and Nb₉₅Cr₀₅ alloys.

There are obvious analogies when Nb is alloyed with its 4d-neighbors (Zr and Mo) with the case of V alloyed with its 3d-neighbors (Ti and Cr) [20]. Addition of 5 at. % of Zr to Nb significantly decreases the total energy of pure Nb mostly due to decrease in ΔE_I (-0.0145 mRy), but also due to decrease in ΔE_M (-0.0079 mRy) resulting, in total, of -0.0224 mRy (~ 21 %) decrease of the total energy, ΔE_{tot} . This is the largest drop of the total energy when Nb is alloyed with the 3d-5d metals under consideration. Adding 5 at.

% of Mo to Nb causes the same effect that is observed in the V-Cr alloy, the ΔE_I (+0.0052) increases and ‘overcomes’ some negative value of ΔE_M (-0.0020 mRy) resulting in a slight ($\Delta E_{tot} = + 0.0032$ mRy) stabilization of the bcc phase in the Nb₉₅Mo₀₅ alloy.

Due to the similarity between $4d$ and $5d$ states, one can explain why an insignificant charge transfer occurs when $4d$ -Nb is alloyed with $5d$ -metals Hf, Ta, and W (see Table 4). Addition of 5 at. % Hf or W decreases the total energy of pure Nb: $\Delta E_{tot} = -0.0155$ mRy and -0.0066 mRy for the Nb₉₅Hf₀₅ and Nb₉₅W₀₅ alloys, respectively, indicating a slight destabilization of the bcc phase. In the case of the Nb₉₅Ta₀₅ alloy the changes in both ΔE_M and ΔE_I are positive: $+0.0020$ mRy and $+0.0005$ mRy, respectively, resulting in a slight ($\Delta E_{tot} = +0.0025$ mRy) stabilization of the bcc phase in the Nb₉₅Ta₀₅ alloy. As both Nb and Ta belong to the Group VB transition metals and Ta belongs to a higher ($5d$ -) series than $4d$ -Nb, we try to find some similarity to the case when another Group VB transition metals, $3d$ -V, is alloyed with a higher $4d$ -metal, Nb, which also belongs to the same Group VB transition metals. There is also a positive charge transfer (0.046) on the Nb atoms in the Nb-Ta equiatomic alloy, which, however, is almost as 5.4 times smaller than that on the V atoms in the V-Nb equiatomic alloy (see Tables 2 and 4). The increase in the electrostatic Madelung energy is proportional to the magnitude of the charge transfer supplied into the interstitial region and it is not surprising that the change in the ΔE_M due to alloying in the V₉₅Nb₀₅ alloy is significantly larger ($+0.0282$ mRy) than for the Nb₉₅Ta₀₅ alloy ($+0.0005$ mRy). The change in ΔE_I is also positive in the case of the V₉₅Nb₀₅ alloy ($+0.0059$ mRy), which is also larger than that in the Nb₉₅Ta₀₅ alloy ($+0.0020$ mRy). Nevertheless, there are obvious similarities between the V₉₅Nb₀₅ and

Nb₉₅Ta₀₅ alloys: the positive charge transfer on the host atoms, the positive band-structure and electrostatic Madelung energy contributions and, as a result, the stabilization of the bcc phase. In fact, only Mo and Ta stabilize the bcc structure in Nb but all the other metals under consideration behave differently where the largest degree of destabilization of the bcc phase in Nb takes place in the Nb-Zr system.

In Ref. [20] we performed calculations of the energy change of pure bcc Ta, and its alloys with 5*d* neighbors (Ta₉₀Hf₁₀, and Ta₉₀W₁₀) caused by 1 % of the monoclinic deformation. The calculations were performed at the same atomic volume $\Omega = 14.68 \text{ \AA}^3$ corresponding to a pressure of ~ 0.65 Mbar, which is within the range of the c_{44} softening (Figure 5), and the results are presented in Table 5. In Table 6 we summarize the calculated charge transfers for Ta alloyed with the members of Group IVB, VB, and VIB. Again, there are analogies to the case of V and Nb when they are alloyed with their nearest neighbors within the same *d*-transition series. Addition of Hf (W) to Ta decreases (increases) ΔE_{tot} due to the corresponding change of the band-structure energy part. The change in ΔE_I due to alloying is -0.0089 mRy and + 0.0080 mRy for the Ta₉₀Hf₁₀, and Ta₉₀W₁₀ alloys, respectively. Similar to V alloyed with its 3*d* neighbors and Nb alloyed with its 4*d* neighbors, the charge transfer on the Ta atoms alloyed with its 5*d* neighbor is very small, 0.044 (Ta-Hf) and -0.051 (Ta-W) for the equiatomic alloys, causing an insignificant change in ΔE_M , +0.0039 mRy due to alloying in the case of the Ta₉₀Hf₁₀ alloy and no change of the same property in the case of the Ta₉₀W₁₀ alloy ($\Delta E_M = 0$). As a result we have a slight decrease in ΔE_{tot} (-0.0050 mRy) when Ta is alloyed with Hf and a slight increase in ΔE_{tot} (+0.0080 mRy) when Ta is alloyed with W. Even though Hf in Ta have a destabilizing effect, the bcc phase always remains stable simply because the

softening in c_{44} in Ta (Figure 5) is not severe enough to promote a phase transition. This fact is also reflected in the larger ΔE_{tot} for Ta compared to that of V and Nb.

Table 5 also contains the results of present calculations for the alloys that Ta forms with $3d$ -metals (Ti, V, and Cr) and $4d$ -metals (Zr, Nb, and Mo). In analogy with Nb, there is a significant negative charge transfer on the host (Ta) atoms, when Ta is alloyed with $3d$ metals (Ti, V, and Cr), that provides a decrease in ΔE_M (-0.0056 mRy, -0.0105 mRy, and -0.0133 mRy for the $Ta_{90}Ti_{10}$, $Ta_{90}V_{10}$, and $Ta_{90}Cr_{10}$ alloys, respectively), which magnitude is proportional to the magnitude of the charge transfer (see Table 6). A decrease in ΔE_I also takes place (-0.0108 mRy, -0.0101 mRy, and -0.0081 mRy for the $Ta_{90}Ti_{10}$, $Ta_{90}V_{10}$, and $Ta_{90}Cr_{10}$ alloys, respectively), but, again as it was in the case of Nb- $3d$ metals based alloys, opposite to ΔE_M behavior: the drop in ΔE_I decreases as the absolute value of the charge transfer on the Ta atoms increases. Consequently, there is a significant decrease (softening) in the total energy change when Ta is alloyed with $3d$ metals (-0.0164 mRy, -0.0206 mRy, and -0.0214 mRy for the $Ta_{90}Ti_{10}$, $Ta_{90}V_{10}$, and $Ta_{90}Cr_{10}$ alloys, respectively). The largest decrease ($\sim 9.9\%$) occurs in the $Ta_{90}Cr_{10}$ alloy corresponding to the greatest negative charge transfer on the Ta atoms. Nevertheless, all these alloys remain stable in the bcc structure due to the large value of ΔE_{tot} in pure Ta.

Finally, when Ta is alloyed with $4d$ -metals (Zr and Mo) the largest drop in ΔE_M due to alloying (-0.0071 mRy) is observed in the $Ta_{90}Mo_{10}$ alloy where a relatively large negative charge transfer on the Ta atoms (-0.127) takes place. For the $Ta_{90}Zr_{10}$ alloy, where the charge transfer on the Ta atoms is positive (+0.041), the change in ΔE_M is positive (+0.0027 mRy). A decrease in ΔE_I also occurs (-0.0143 mRy and -0.0050 mRy

for the Ta₉₀Zr₁₀ and Ta₉₀Mo₁₀ alloys, respectively). This situation is similar to that when Ta is alloyed with 3*d*-metals: the drop in ΔE_I decreases as the absolute value of the charge transfer on the Ta atoms increases. The decrease in both ΔE_I and ΔE_M in the Ta₉₀Mo₁₀ alloy and a significant decrease in ΔE_I , which overcomes a slight increase in ΔE_M in the Ta₉₀Zr₁₀ alloy, result in a decrease in the total energy in the Ta₉₀Mo₁₀ and Ta₉₀Zr₁₀ alloys (-0.0121 mRy and -0.0116 mRy, respectively) still leaving both alloys stable in the bcc structure.

Alloying Ta with 10 at. % of Nb increases ΔE_M (+0.0066 mRy) and decreases ΔE_I (-0.0023 mRy) resulting in increase of the total energy, ΔE_{tot} , (+ 0.0043 mRy). The increase in ΔE_M occurs in spite of the small but negative charge transfer on the Ta atoms (-0.046). These values are numerically very small and represent an exception to the rule of thumb we have discovered: the sign (positive or negative) of the change of the ΔE_M due to alloying of two transition metals from the different *d*-series corresponds to the sign (positive or negative) of the charge transfer on the host atoms. As a result, Nb joins W as the only metals under consideration that stabilize the bcc structure of Ta.

V. DISCUSSION AND CONCLUSIONS

In our previous papers [9, 10] we established that softening in the shear constants of V and Nb under compression, is entirely due to the band-structure peculiarities, namely to the FS nesting, ETT, and band J-T effects. It was also established that the nesting vector spanning two flat pieces of the FS already exists at ambient pressure and leads to the Kohn anomaly on the transverse acoustic phonon mode TA [ξ 00]. Reliable data on the phonon dispersions for V became recently available [1], and it is now possible

to verify predictions made in Refs. [9, 10]. In the present study we prove that the length of the above mentioned nesting vector, defined as the peak in the generalized susceptibility curve calculated at ambient pressure, matches the position where the Kohn anomaly (the maximum deviation from the elastic constant line) on the experimental TA $[\xi 00]$ phonon branch occurs. Our calculations confirm that this anomaly takes place at $\xi \approx 0.24, 0.16,$ and 0.28 for V, Nb, and Ta, respectively, in good accord with experimental observations, although the Kohn anomaly is less significant for Ta.

Our present study substantially increases our understanding of what happens with the phase stability of the Group VB (V, Nb, and Ta) transition metals when they are alloyed with each other, their neighbors to the left (Ti, Zr, or Hf) or to the right (Cr, Mo, or W). We have already established in Ref. [20] that the nearest neighbors, within the same d -transition series, with less (to the left) or more (to the right) d -electrons destabilize and stabilize the bcc phase relatively to the low-symmetry rh phase, respectively. We have also stated [20] that when $3d$ vanadium is alloyed with neighbors of a higher d -transition series, Zr, Nb, Mo, Hf, Ta, and W, the electrostatic Madelung energy dominates and promotes stabilization of the bcc phase. We have found that the maximum instability (in the vicinity of 240 GPa) of the bcc vanadium in respect to the low-symmetry rh structure can be removed by addition of $\sim 3 - 5$ at. % of Zr, Nb, Mo, Hf, Ta, or W. We have previously [20] analyzed the relative contributions to the total energy, ΔE_I and ΔE_M , for the $V_{95}Nb_{05}$ alloy in detail. Similar analysis of the remaining V-based alloys not listed in Table 1 of Ref. [20] shows that the band-structure energy contribution also promotes stabilization of the bcc structure and becomes compatible to

the magnitude of the Madelung energy contribution in the case of the V-Mo and V-W alloys and even dominates in the case of the V-Ta alloy.

We have explained that the Madelung energy of the dilute alloy is increasing (decreasing) with the positive (negative) charge transfer on the host atoms and promoting (demoting) the stability of the bcc phase. Primarily this happens when orbitals with different quantum number belong to the constituents of the alloy. There is, however, another effect that may be playing a lesser role. In Table 7 we show the measured (room temperature [37]) and calculated (EMTO) equilibrium Wigner-Seitz radii of the studied elements. It is evident that the $3d$ elements have the smaller atomic volume (or radius) than the $4d$ and $5d$ elements. This difference can influence the charge transfer between the constituents of the alloy or, using the terminology of Ref. [25], the ‘net charge’ that originates from the redistribution of the electron density in the interstitial region between the atomic spheres.

Nb and W as the only metals under consideration that stabilize the bcc structure of Ta. Both Ta-Nb and Ta-W alloys have unlimited range of the bcc solid solutions [38, 39]. It is well known that impurities and alloying can have a profound influence on the yield strength properties of a material [40]. Schwartz *et al.* [41] showed that adding 10 wt. % (9.86 at. %) of W to Ta increases the yield strength of the materials, i.e. the minimum stress that is required to induce the plastic deformation, by more than a factor of two. This observation was confirmed by Yang *et al.* [40] who calculated the elastic constants of the $\text{Ta}_{100-x}\text{W}_x$ alloys and successfully reproduced the experimental concentration behavior of the trigonal shear elastic constant, c_{44} [42]. Our calculations also confirm a gradual increase of the trigonal shear elastic constant, c_{44} , of the $\text{Ta}_{100-x}\text{W}_x$ alloys together

with W content observed in Ref. [42]. We also found a similar behavior in the $\text{Ta}_{100-x}\text{Nb}_x$ alloys as the amount of Nb in the alloy increases, but this result requires experimental confirmation. If our results are true, we recommend alloying Ta with Nb for strengthening.

To summarize, we have identified that the band-structure structure peculiarities are responsible for the Kohn anomaly on the transverse acoustic phonon mode TA [$\xi 00$] of the Group VB transition metals and softening in their shear elastic constant with pressure. For V this softening is associated with a phase transition to a rhombohedral phase close to 60 GPa while for Nb and Ta the bcc phase still remains stable at all studied pressures. The effect of alloying on the phase stability has been studied and three dominant mechanisms are recognized. First, the band-structure energy tends to destabilize or stabilize the bcc phase when a member of the Group VB is alloyed with its nearest neighbor from the same d -transition series to left or to the right, respectively. Second, the increase in both the electrostatic Madelung and band-structure energies remove softening and secure the bcc phase when vanadium metal is alloyed with neighboring elements from a higher d -transition series. Third, the decrease in both the electrostatic Madelung and band-structure energies causes some destabilization of the bcc phase when niobium or tantalum metals are alloyed with neighboring elements from the $3d$ -transition series although this destabilization is too small to cause a phase transition. Finally, a slight destabilization of the bcc phase occurs when niobium metal is alloyed with Hf or W or when tantalum metal is alloyed with Zr and Mo but both Nb and Ta remain stable in the bcc structure. The stability of the bcc phase is only strengthened

when the ‘mixed’ (*4d* and *5d*) alloy has components from the same Group VB (the Nb-Ta system).

ACKNOWLEDGEMENTS

Work performed under the auspices of the US DOE by LLNL under contract DE-AC52-07NA27344. Support from the Swedish Research Council (VR) is gratefully acknowledged by AVR, OEP, and LV. AL Would like to acknowledge A. Bosak for providing numerical data on the TA [$\xi 00$] phonon branch for vanadium metal.

References

1. A. Bosak, M. Hoesch, D. Antonangeli, D.L. Farber, I. Fischer, and M. Krisch, Phys. Rev. B **78** (2008) 020301(R).
2. N. Suzuki and M. Otani, J. Phys.: Condens. Matter **14** (2002) 10869; *ibid.* **19** (2007) 125206.
3. W. Luo, R. Ahuja, Y. Ding, and H.K. Mao, Proc. Natl. Acad. Sci. **104** (2007) 16428.
4. A.K. Verma and P. Modak, Europhys. Lett. **81** (2008) 37003.
5. M. Ishizuka, M. Iketani, and S. Endo, Phys. Rev. B **61** (2000) 3823.
6. Y. Ding, R. Ahuja, J. Shu, P. Chow, W. Luo, and H.K. Mao, Phys. Rev. Lett. **98** (2007) 085502.
7. B. Lee, R.E. Rudd, J.E. Klepeis, P. Söderlind, and A. Landa, Phys. Rev. B **75** (2007) 180101(R).
8. S.L. Qui and P.M. Marcus, J. Phys.: Condens. Matter **20** (2008) 275218.

9. A. Landa, J. Klepeis, P. Söderlind, I. Naumov, O. Velikokhatnyi, L. Vitos, and A. Ruban, *J. Phys.: Condens. Matter* **18** (2006) 5079.
10. A. Landa, J. Klepeis, P. Söderlind, I. Naumov, O. Velikokhatnyi, L. Vitos, and A. Ruban, *J. Phys. Chem. Sol.* **67** (2006) 2056.
11. L. Koči, Y. Ma, A.R. Oganov, P. Souvatzis, and R. Ahuja, *Phys. Rev. B* **77** (2008) 214101.
12. A. Wexler and W.S. Corak, *Phys. Rev.* **85** (1952) 85.
13. V.V. Struzhkin, Y.A. Timofeev, R.J. Hemley, and H.K. Mao, *Phys. Rev. Lett.* **24** (1997) 4262.
14. B.T. Matthias, T.H. Geballe, and V.B. Compton, *Rev. Mod. Phys.* **35** (1) (1963) 1.
15. Y. Nakagawa and A.D.B. Woods, *Phys. Rev. Lett.* **11** (1963) 271.
16. R.I. Sharp, *J. Phys. C: Solid St. Phys.* **2** (1969) 421, *ibid.* **2** (1969) 432.
17. C.M. Varma and W. Weber, *Phys. Rev. B* **19** (1979) 6142.
18. A.D.B. Woods, *Phys. Rev.* **136** (1964) A781.
19. F. Sacchetti, C. Petrillo, and O. Moze, *Phys. Rev. B* **49** (1994) 8747.
20. A. Landa, P. Söderlind, A.V. Ruban, O.E. Peil, and L. Vitos, *Phys. Rev. Lett.* **103** (2009) 235501.
21. L. Vitos, *Computational Quantum Mechanics for Materials Engineers: The EMTO Method and Applications* (Springer-Verlag, London, 2007).
22. J.P. Perdew, K. Burke, and Ernzerhof, *Phys. Rev. Lett.* **77** (1996) 3865.
23. J. S. Faulkner, *Prog. Mat. Sci.* **27** (1982) 1.

24. D.J. Chadi and M.L. Cohen, Phys. Rev B **8** (1973) 5747; S. Froyen, *ibid.* **38** (1989) 3168.
25. A.V. Ruban and H. L. Skriver, Phys. Rev. B **66** (2002) 024201; A.V. Ruban, S.I. Simak, P.A. Korzhavyi, and H.L. Skriver, *ibid.* **66** (2002) 024202.
26. I.A. Abrikosov, S.I. Simak, B. Johansson, A.V. Ruban, and H.L. Skriver, Phys Rev. B **56** (1997) 9319.
27. F. D. Murnaghan, Proc. Natl. Acad. Sci. **30** (1944) 244.
28. M. Mehl, B.M. Klein, and D.A. Papaconstantopoulos, in: *Intermetallic Compounds: Principles and Practice, vol. 1 Principles*, edited by J.H. Westbrook and R.L. Fleisher (Wiley, London, 1995), p. 195.
29. J. Rath and A.J. Freeman, Phys. Rev. B **11** (1975) 2109.
30. J.M. Wills, O. Eriksson, M. Alouani, and D.L. Price, in: *Electronic Structure and Physical Properties of Solids*, edited by H. Dreysee (Springer-Verlag, Berlin, 1998), p. 148.
31. A. Bosak, private communication (2010).
32. B. M. Powell, R. Martel, and A.D.B. Woods, Phys. Rev. **171** (1968) 171; Can. J. Phys. **55** (1977) 1601.
33. M.I. Katsnelson, I. I. Naumov, and A.V. Trefilov, Phase Transit. **49** (1994) 143.
34. P. Söderlind and J.M. Moriarty, Phys. Rev. B **57** (1998) 10340.
35. R. Cohen and O. Gülseren, Phys. Rev. B **63** (2001) 224101.
36. O. Gülseren and R. Cohen, Phys. Rev. B **65** (2002) 064103.
37. H.L. Skriver, *The LMTO Method* (Springer-Verlag, Berlin, 1984) p. 262.

38. R. Krishnan, S.P. Garg, and N. Krishnamurthy, Nb-Ta (Niobium-Tantalum), in: *Binary Alloy Phase Diagrams, II Ed.*, edited by T.B. Massalski, Vol. 3 (1990), p. 2772.
39. R. Krishnan, S.P. Garg, and N. Krishnamurthy, Ta-W (Tantalum-Tungsten), in: *Binary Alloy Phase Diagrams, II Ed.*, edited by T.B. Massalski, Vol. 3 (1990), p. 3438.
40. L. Yang, H. Cynn, J.-H. Klepeis, J. Pask, and R. Rudd, in: Abstracts of 2010 March APS Meeting (Portland, OR), Bulletin of the APS 55 No 2 p. 389.
41. A.J. Schwartz, D.H. Lassila, and M.M. LeBlanc, Mater. Sci. and Eng. **A244** (1998) 178.
42. C.E. Anderson and F.R. Brotzen, J. Appl. Phys. **53**(1) (1982) 292.

Captions

Figure 1. Partial ($3^{\text{rd}} \rightarrow 3^{\text{rd}}$ intra-band transition) electron susceptibility of V, Nb, and Ta calculated along the Γ - H direction at ambient pressure.

Figure 2. The experimental phonon dispersion TA curve in $[\xi 00]$ direction for a) V (Ref. [31]), b) Nb (Ref. [32]), and c) Ta (Ref. [19]). The arrow indicates the Kohn anomaly obtained from *an initio* calculations.

Figure 3. Partial ($3^{\text{rd}} \rightarrow 3^{\text{rd}}$ intra-band transition) electron susceptibility of a) V, b) Nb, and c) Ta calculated along the Γ - H direction at a function of pressure.

Figure 4. The magnitude of the nesting vector for V, Nb, and Ta as a function of pressure.

Figure 5. Calculated pressure dependence of the trigonal shear elastic constant in V, Nb, and Ta [20].

Figure 6. Calculated total energy (at the atomic volume $\Omega = 8.056 \text{ \AA}^3$) as a function of the rhombohedral deformation parameter δ (see Ref. [7] for explanation) [20]. The undistorted ($\delta = 0$) crystal corresponds to the bcc phase. The curves for $\text{V}_{95}\text{Ti}_{05}$, $\text{V}_{95}\text{Cr}_{05}$, and $\text{V}_{95}\text{Nb}_{05}$ are shifted apart 50 mRy for a better display of the results.

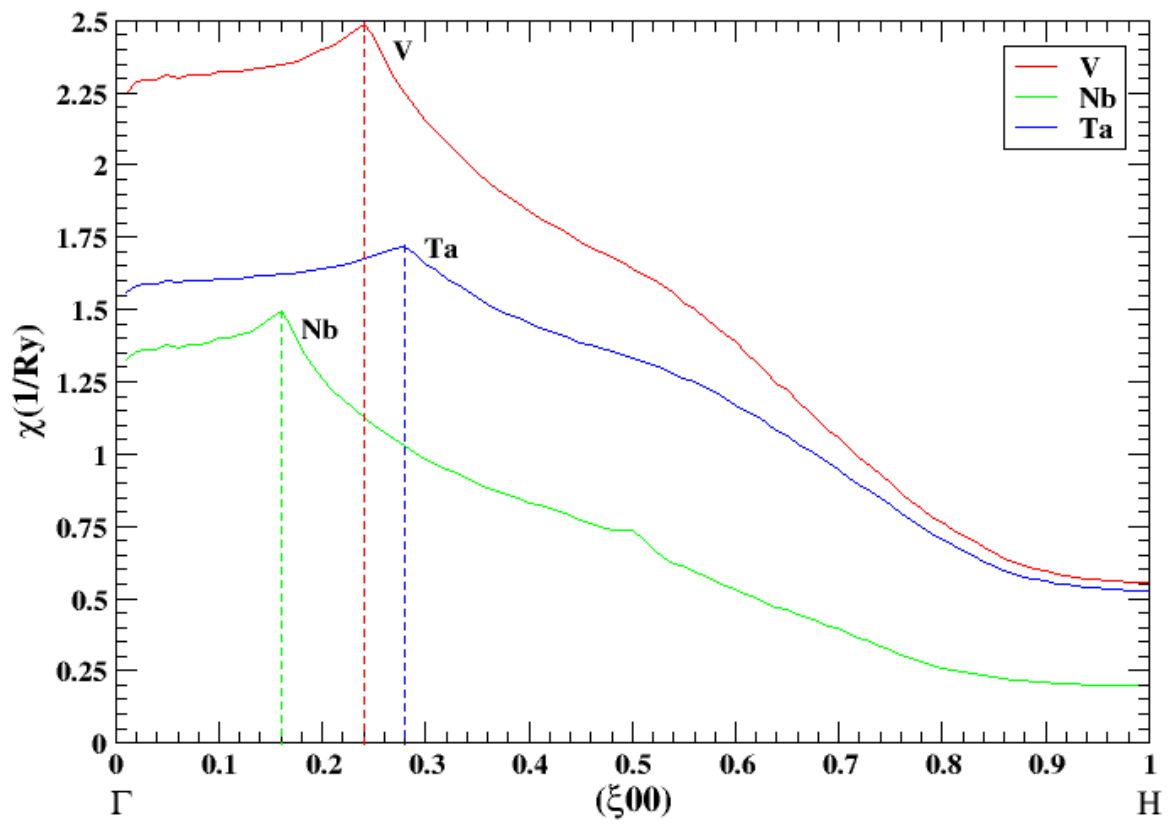


Figure 1.

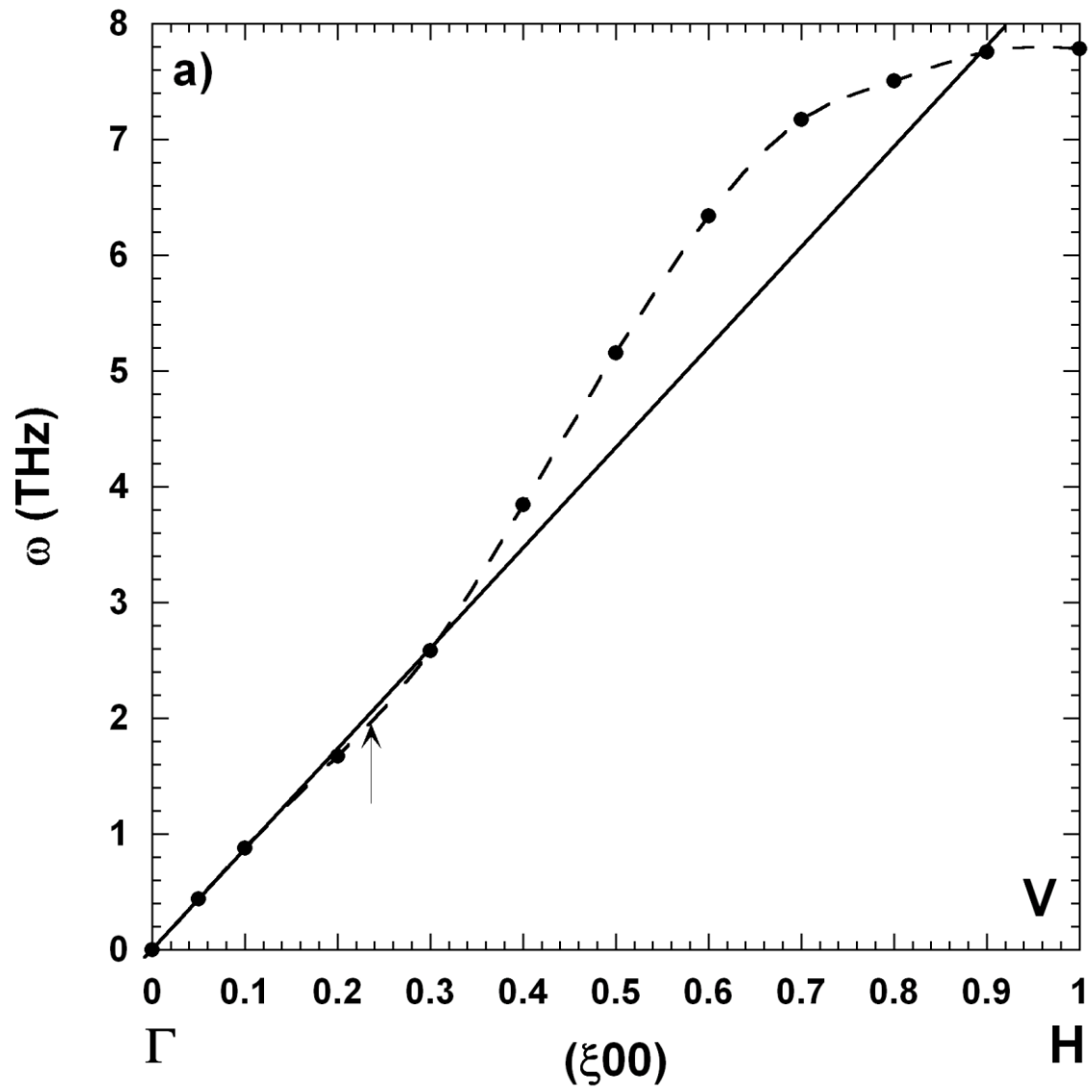


Figure 2a.

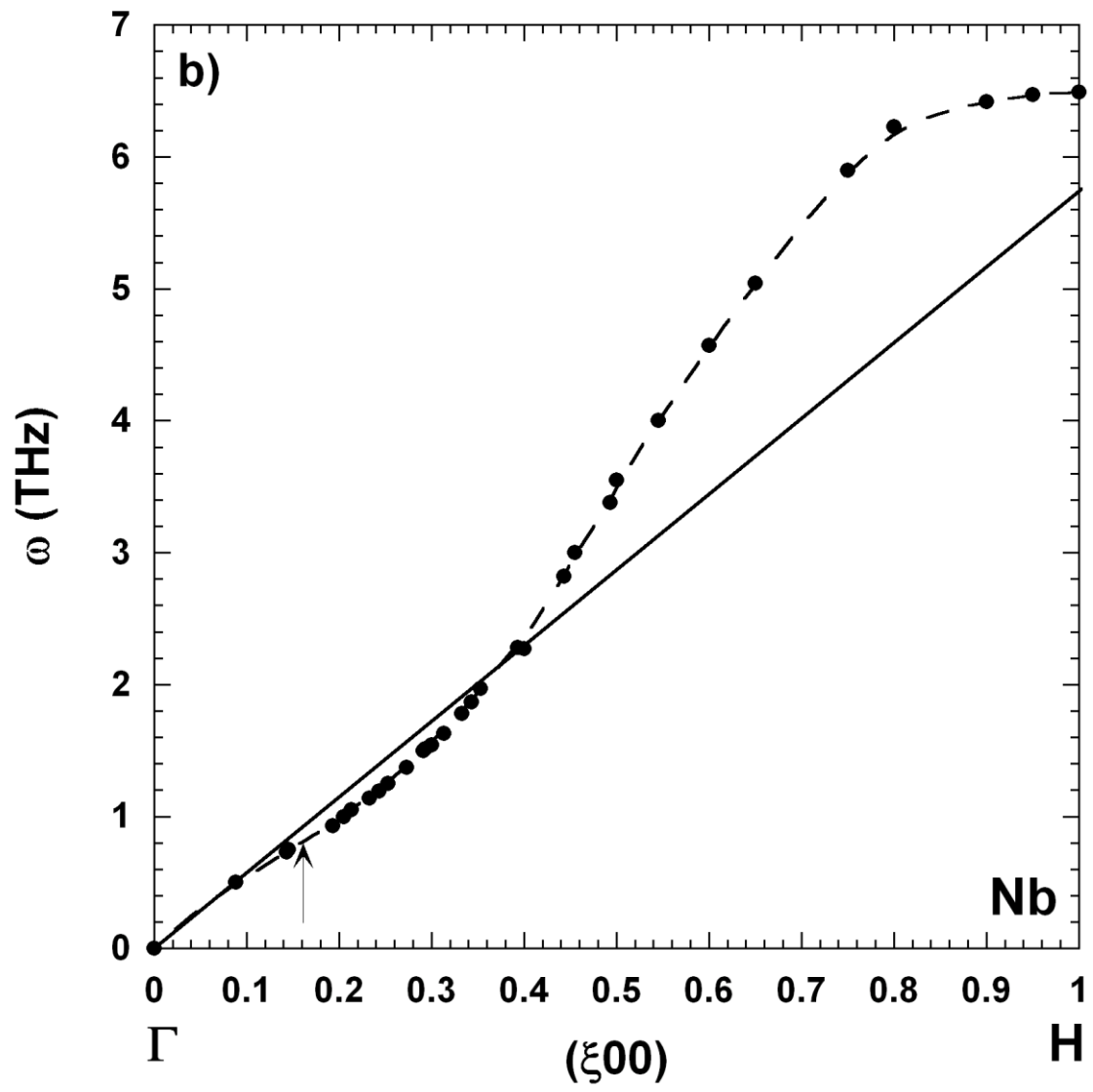


Figure 2b.

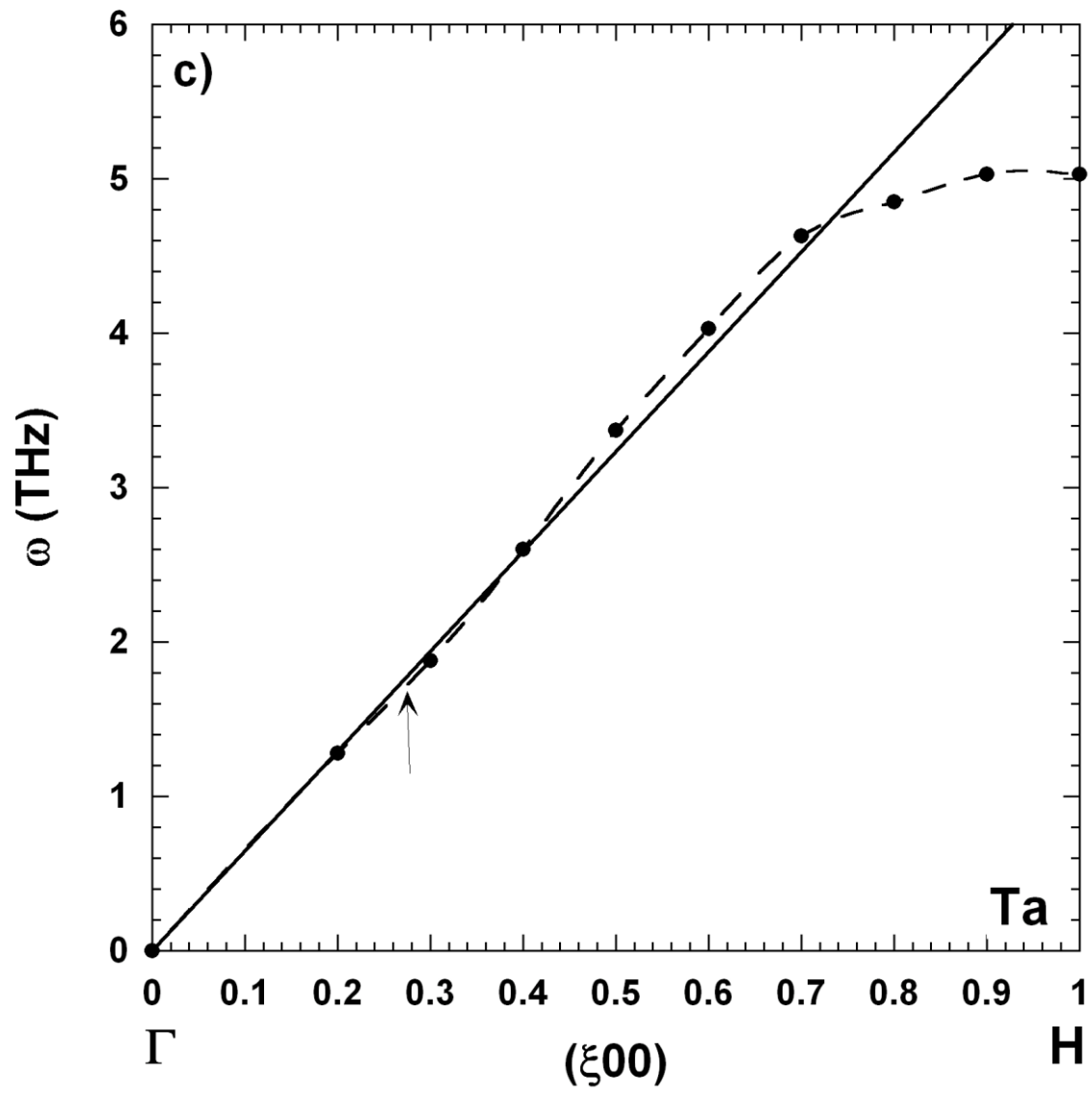


Figure 2c.

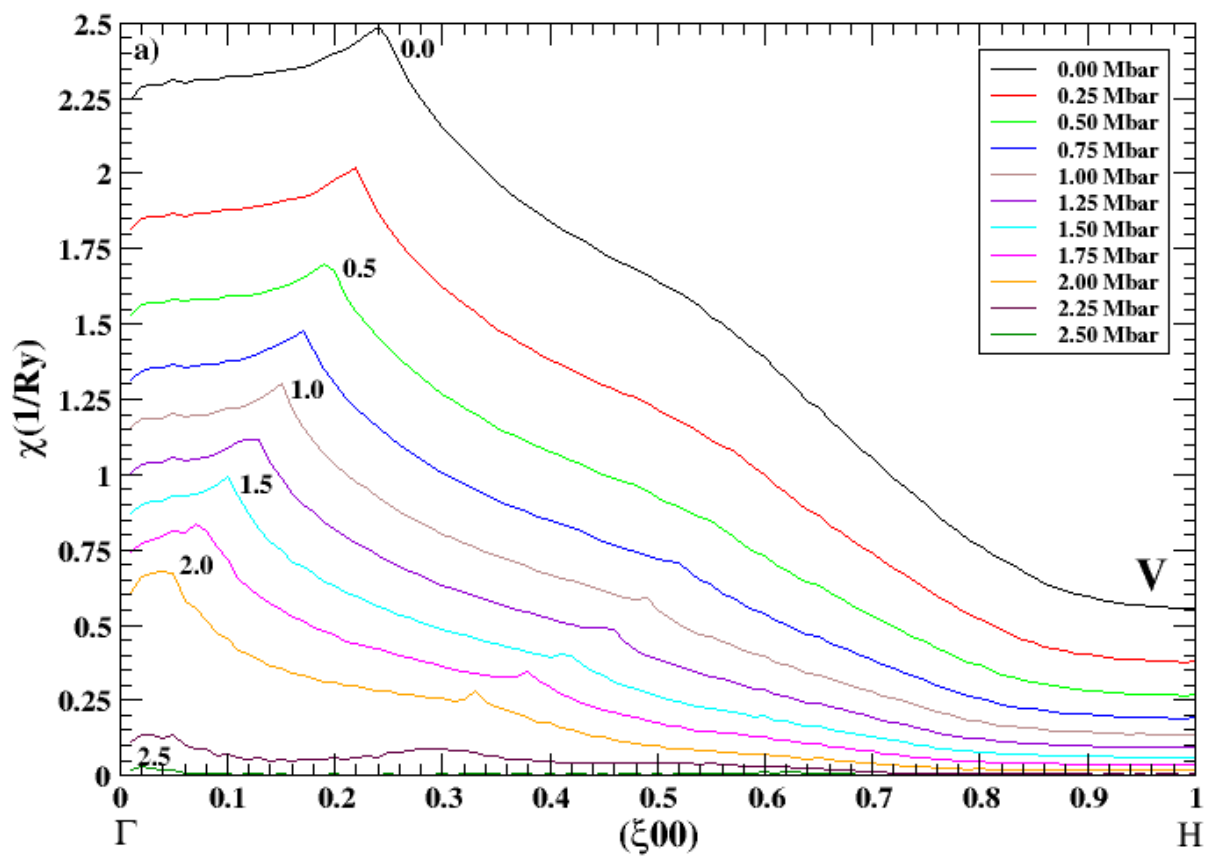


Figure 3a.

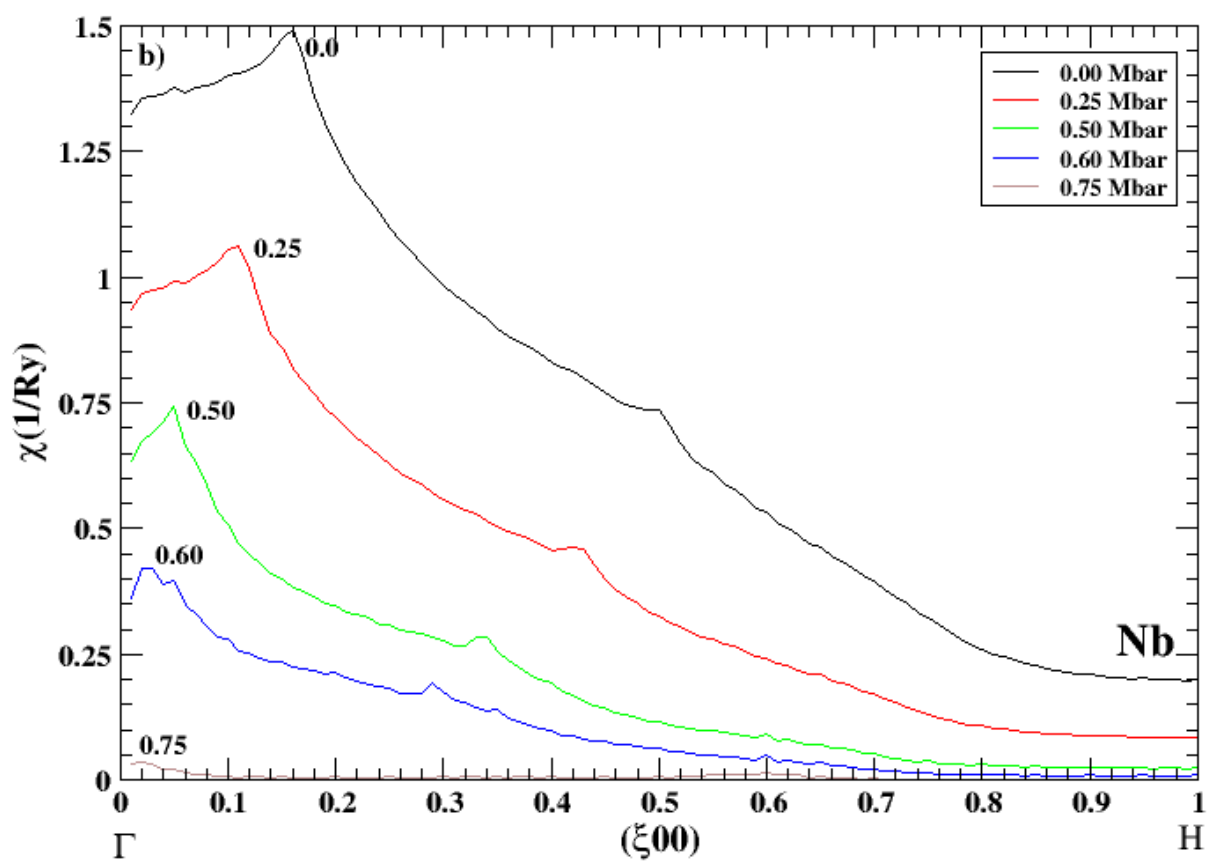


Figure 3b.

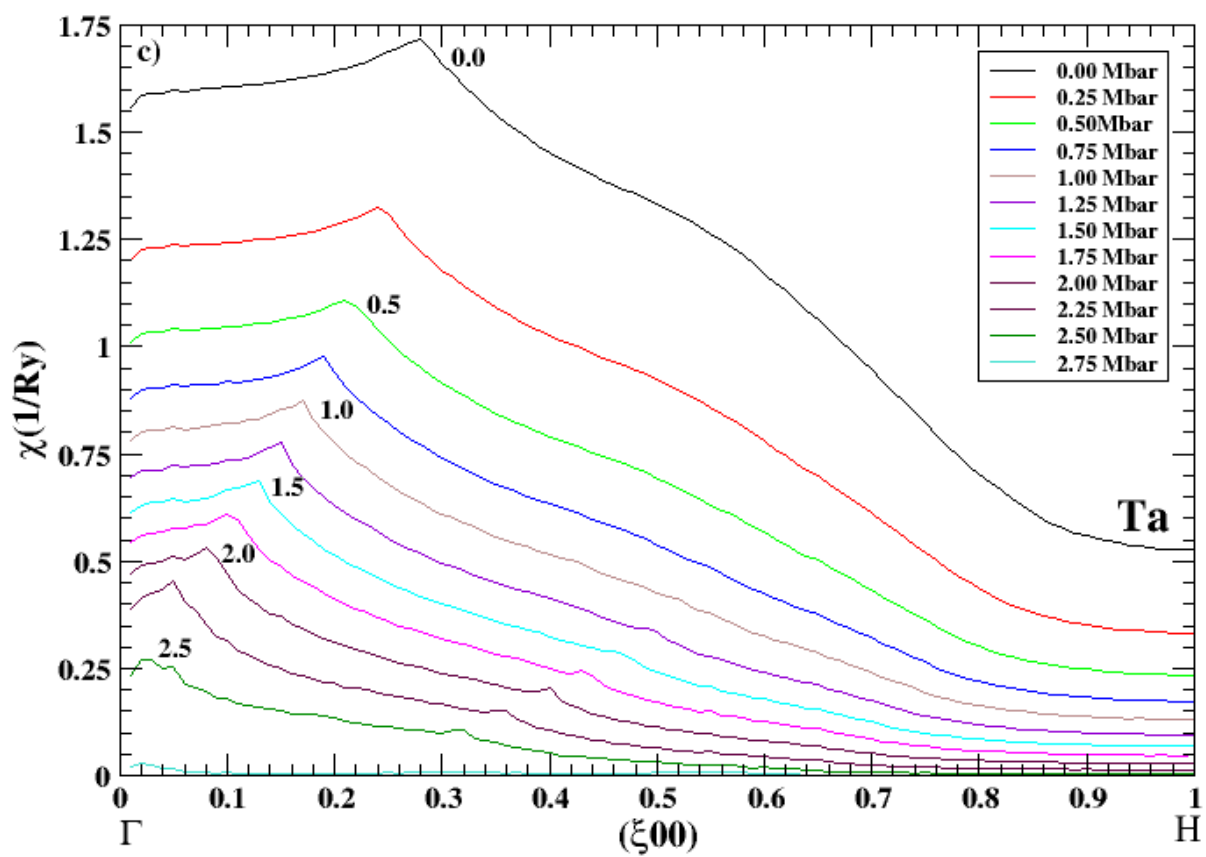


Figure 3c

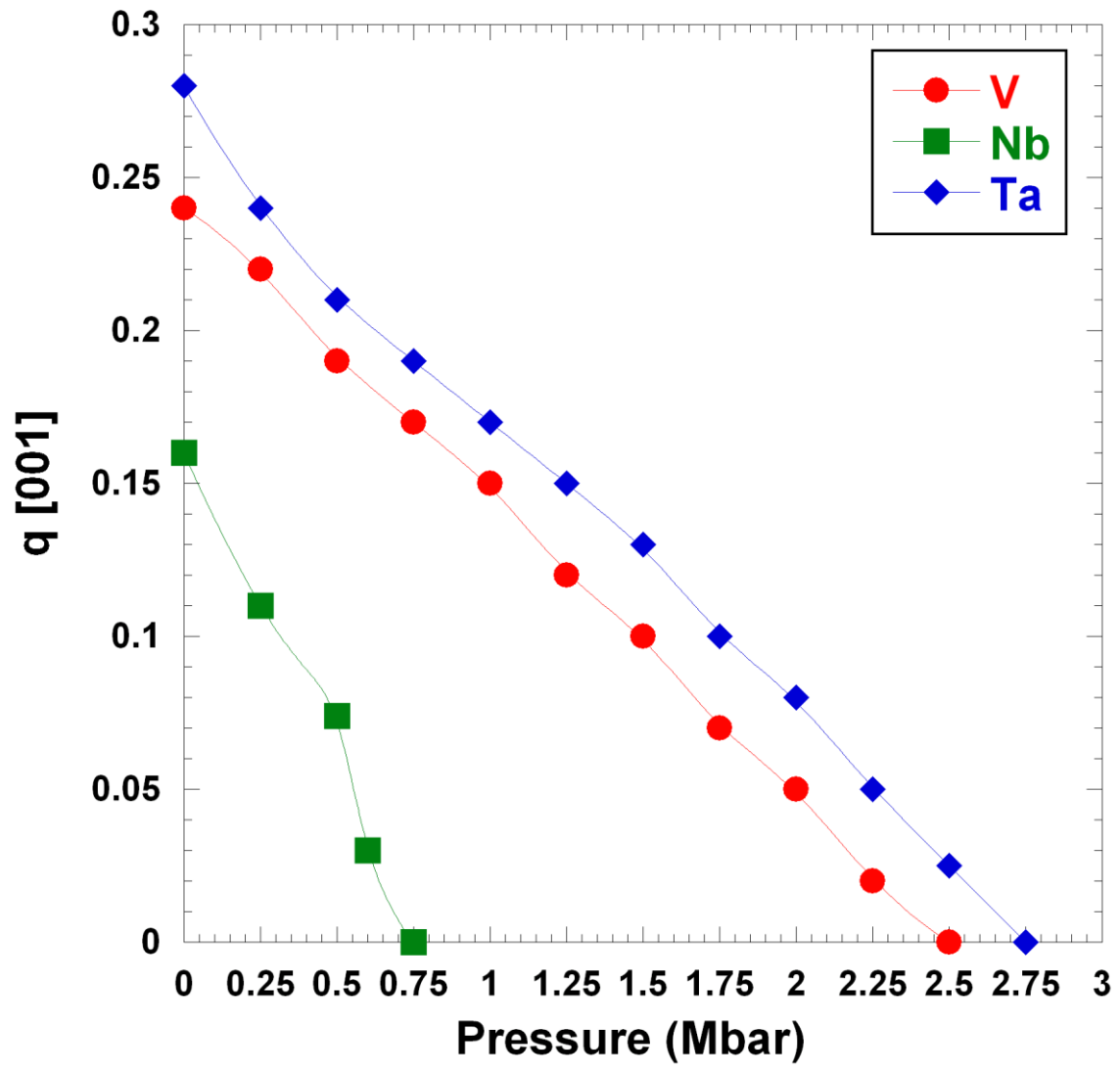


Figure 4.

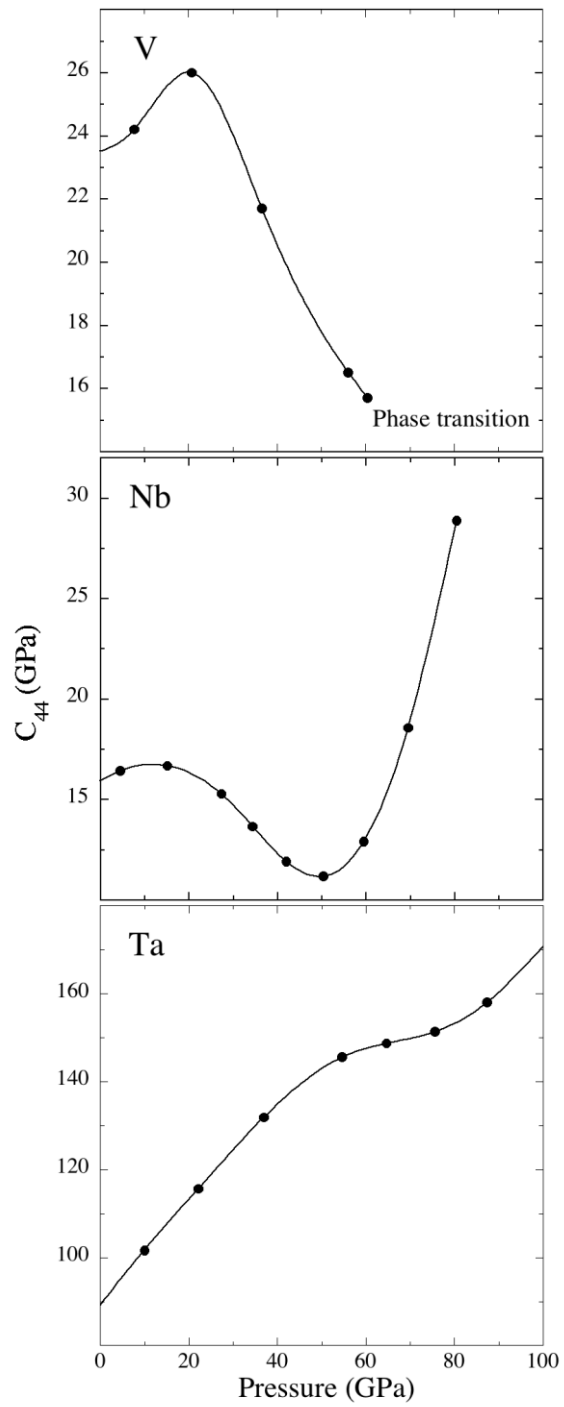


Figure 5.

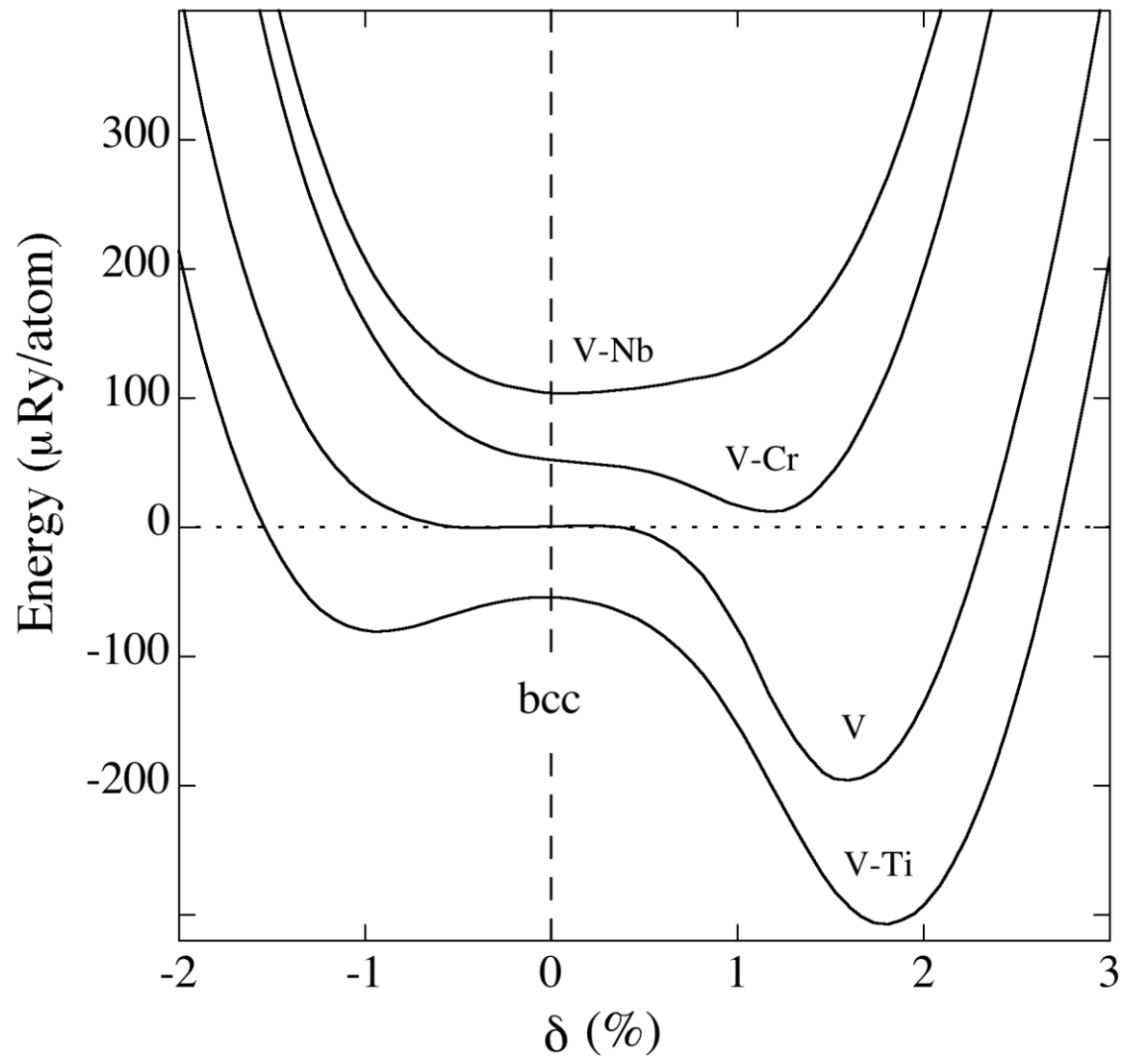


Figure 6.

Tables.

Table 1. Contributions to the total-energy change (ΔE_{tot}) due to a 1 % monoclinic deformation for V and its alloys.

Material	ΔE_I (mRy)	ΔE_M (mRy)	ΔE_{tot} (mRy)
V	-0.2010	0.1820	-0.0190
V ₉₅ Ti ₀₅	-0.2130	0.1895	-0.0235
V ₉₅ Cr ₀₅	-0.1887	0.1823	-0.0064
V ₉₅ Zr ₀₅	-0.1864	0.2121	0.0257
V ₉₅ Nb ₀₅	-0.1951	0.2102	0.0151
V ₉₅ Mo ₀₅	-0.1855	0.1939	0.0084
V ₉₅ Hf ₀₅	-0.1931	0.2044	0.0113
V ₉₅ Ta ₀₅	-0.1662	0.2003	0.0341
V ₉₅ W ₀₅	-0.1150	0.1915	0.0765

Table 2. The calculated charge transfer induced on the V atoms in V-M alloys.

V-Ti (0.077)	V-V (0.000)	V-Cr (-0.070)
V-Zr (0.290)	V-Nb (0.247)	V-Mo (0.196)
V-Hf (0.306)	V-Ta (0.296)	V-W (0.277)

Table 3. Contributions to the total-energy change (ΔE_{tot}) due to a 1 % monoclinic deformation for Nb and its alloys.

Material	ΔE_I (mRy)	ΔE_M (mRy)	ΔE_{tot} (mRy)
Nb	-0.0860	0.1930	0.1070
Nb ₉₅ Ti ₀₅	-0.0940	0.1839	0.0899
Nb ₉₅ V ₀₅	-0.0905	0.1829	0.0924
Nb ₉₅ Cr ₀₅	-0.0896	0.1786	0.0890
Nb ₉₅ Zr ₀₅	-0.1005	0.1851	0.0846
Nb ₉₅ Mo ₀₅	-0.0808	0.1910	0.1102
Nb ₉₅ Hf ₀₅	-0.0946	0.1861	0.0915
Nb ₉₅ Ta ₀₅	-0.0840	0.1935	0.1095
Nb ₉₅ W ₀₅	-0.0846	0.1850	0.1004

Table 4. The calculated charge transfer induced on the Nb atoms in Nb-M alloys.

Nb-Ti (-0.146)	Nb-V (-0.247)	Nb-Cr (-0.336)
Nb-Zr (0.084)	Nb-Nb (0.000)	Nb-Mo (-0.081)
Nb-Hf (0.088)	Nb-Ta (0.046)	Nb-W (-0.005)

Table 5. Contributions to the total-energy change (ΔE_{tot}) due to a 1 % monoclinic deformation for Ta and its alloys.

Material	ΔE_I (mRy)	ΔE_M (mRy)	ΔE_{tot} (mRy)
Ta	-0.0080	0.2250	0.2170
Ta ₉₀ Ti ₁₀	-0.0188	0.2194	0.2006
Ta ₉₀ V ₁₀	-0.0181	0.2145	0.1964
Ta ₉₀ Cr ₁₀	-0.0161	0.2117	0.1956
Ta ₉₀ Zr ₁₀	-0.0223	0.2277	0.2054
Ta ₉₀ Nb ₁₀	-0.0103	0.2316	0.2213
Ta ₉₀ Mo ₁₀	-0.0130	0.2179	0.2049
Ta ₉₀ Hf ₁₀	-0.0169	0.2289	0.2120
Ta ₉₀ W ₁₀	0.0000	0.2250	0.2250

Table 6. The calculated charge transfer induced on the Ta atoms in Ta-M alloys.

Ta-Ti (-0.193)	Ta-V (-0.296)	Ta-Cr (-0.386)
Ta-Zr (0.041)	Ta-Nb (-0.046)	Ta-Mo (-0.127)
Ta-Hf (0.044)	Ta-Ta (0.000)	Ta-W (-0.051)

Table 7. Equilibrium Wigner-Seitz radius (EMTO) of bcc metals. Experimental data at room temperatures are shown in parentheses [37]. Notice that experimental data for the Group IVB metals (Ti, Zr, and Hf) correspond to the hcp structure.

Ti 3.035 (3.052)	V 2.799 (2.818)	Cr 2.655 (2.684)
Zr 3.334 (3.347)	Nb 3.089 (3.071)	Mo 2.949 (2.922)
Hf 3.298 (3.301)	Ta 3.115 (3.069)	W 2.976 (2.945)